Effect of size and light power on the fluorescence yield of rubrene nanocrystals

Guillaume J. Laurent, N.Thanh Ha-Duong, Rachel Méallet-Renault, Robert Bernard Pansu

? Chapter 00 ?

Effect of size and light power on the fluorescence yield of rubrene nanocrystals.

G. Laurent, N. T. Ha-Duong, R. Méallet-Renault, R. B. Pansu

Laboratoire de Photophysique et Photochimie Supramoléculaires et Macromoléculaires
UMR CNRS 8531, Ecole Normale Supérieure de Cachan.
61, avenue du président Wilson ; 94235 Cachan cedex ; France.
pansu@ppsm.ens-cachan.fr

Keywords : rubrene, organic nanocrystals, fluorescent nanoparticles.

Abstract :
Rubrene nanocrystals are fluorescent. They exhibit a fluorescent lifetime of 16.4 ns, close to the natural lifetime, but a fluorescence yield of only 8 %. We have studied the size effect on fluorescence yield. Rubrene nanocrystals were prepared by flash evaporation of toluene from an emulsion. The size distribution of nanocrystals peaks between 50 and 500 nm depending on the toluene to water ratio. The colloidal dispersion of nanoparticles is stable for months. Size dependence was studied by filtration. The fluorescence yield increases sharply below 50 nm from 0.08 to 0.7. This effect is attributed to the presence of impurities in the crystals. The impurities quench their surroundings. As the crystal is fragmented, the quenching is confined to smaller volumes. An increase of the fluorescence yield is observed. Excited states can also act as quenchers for the fluorescence in a nanocrystal. Increasing the laser power in a confocal set-up leads to a saturation of the fluorescence and a reduction of its lifetime.

1. INTRODUCTION

The preparation and properties of fluorescent micro- and nanoparticles have recently given rise to number of studies. For instance, nanoparticles of metals and inorganic semiconductors are investigated from a fundamental point of view (quantum confinement) and also for applications in nonlinear optics [1],2]. Their good photostability and long fluorescence lifetime make them appropriate labels

for long term labelling [3]. Some quantum dots were also designed to be biocompatible [4, 5]. Highly fluorescent nanoparticles are also highly desirable for superamplified biochemical assays [6, 7].
Concerning luminescent organic particles a burst occurred a few years ago. They can be used as organic electroluminescent diodes [8]. Fluorescent organic nanocrystals synthesis have been reported using reprecipitation method [9,10,11], and microwave irradiation [12, 13]. Crystal size dependence of spectroscopics properties were found. For instance, fluorescence spectra of perylene nano- and microcrystals were found to be dependent of particles size. The emission peak of self-trapped exciton is shifted to blue with decreasing size [14, 15]. Absorption and emission properties can be size-tunned in several pyrazolines molecules [10, 16, 17].
Controlled growth and stabilization of fluorescent organic nanocrystals were studied in sol-gel matrices [18, 19] and in dendrimers [11]. Some studies focussed on polymer and latex particles [20,21] where they have been functionalized into nanosensors. A great interest is focussed on nanosensors since then can be cell-injected or transfected. Luminescent nanocrystals have numerous advantages. Among them we can underline their brigthness, and energy transfer can occur within the particle leading to a high sensitivity. Indeed, compared to molecular sensors, nanoparticles are brighter. For instance a nanocrystal consists of a few tens or a few thousands of chromophores per nm^2. Then the photon capture probability is much bigger than for a single molecule. For excitation under a microscope, nanocrystals, as nanosensors, are much more useful than single molecular sensors because their size is more adaptated. The signal to noise ratio is better. Many applications, such as living cells studies, 100 μm pixel of bio-chips, chamber cells sorter, need quite a big observation volume (compared to SNOM).
The second main advantage of fluorescent nanocrystals is the existence of energy tranfer within the particles. Such antenna effect, in condensed media, was studied by Th. Förster [22]. Such exciton transfer could be useful for quenching studies. If the crystal is smaller than Förster radius, then one acceptor molecule could quench the whole crystal fluorescence. Then sensitivity could be hundred times higher than for single molecular sensors.
Other nanoparticles exhibit antenna effect and have been used as nano-sensors : dendrimers [23], luminescent conducting polymers [24], J-aggregates [25], zeolithes [26].
Among organic molecules, we have firstly chosen CMONS nanocrystals [27]. A size-dependence was observed : lifetime is about few nanoseconds in microcrystals, and decreases to 200 ps in nanocrystals. In this study, we have chosen rubrene (5, 6, 11, 12 – tetraphenylnaphtacene) which is fluorescent in crystalline state. Rubrene is used in LED as an emission center, high rubrene

molar fraction can be used without self-quenching effect [28], the emission from aggregates, after 2-photon excitation have been studied [29].

2. MATERIALS AND METHOD

2.1. Materials

99 % of purity rubrene and spectroscopic grade toluene were purchased from Aldrich. CethylTrimethylAmmonium Chloride (CTACl) was purchased from Acros Organics. No further purifications were done. Distilled and deionised water was used for dilution. MF-Millipore™ Cellulose ester membrane filters of calibrated porosity (0.80, 0.45, 0.22, 0.05, 0.025 μm) were used for filtration. For 0.1 μm pore size, Isopore™ filters were used ; their membrane is made of polycarbonate (Millipore©).

2.2. Steady-state measurements

A U.V.-vis. Varian CARY 500 spectrophotometer was used. Excitation and emission spectra were measured on a SPEX Fluorolog-3 (Jobin-Yvon). A right-angle configuration was used. Optical density of the samples was checked to be less than 0.1 to avoid reabsorption artefact. Signal was corrected from lamp fluctuations.

2.3. Time-resolved spectroscopy

The fluorescence decay curves were obtained with a time-correlated single-photon-counting method using a titanium-sapphire laser (82 MHz, repetition rate lowered to 4 MHz thanks to a pulse-peaker, 1 ps pulse width, a doubling crystal is used to reach 495 nm excitation) pumped by an argon ion laser [30] .

2.4. Preparation of nanocrystals

The rubrene dye was dissolved in toluene (2 % weight *i.e* 10^{-5} mol.L^{-1}). The aqueous CTACl solution was 0.2 mol.L^{-1}. The two solutions were mixed at different ratio of toluene to CTACl solution : 1/1, 1/3, 1/10, 1/30. Sonication and flash evaporation were performed. Four different “mother” suspensions of rubrene crystals in water were thus obtained.

3. RESULTS

3.1. Size control : Size distributions of nanocrystals

Each "mother" suspension was diluted 200 times and then filtered on nominal pore size filters, decreasing the pore size at each step (from 0.8 µm to 0.025 µm). We have checked that the loss of material on the filter was negligible and that repetitive filtration, on fresh filters, of a filtered solution did not induce a significant loss of material. Presence of nanocrystals, in solution, was confirmed at each step by the measurements of absorption and fluorescence spectra measurements (fig. 1.a and 1.b). Absorbance and fluorescence intensity decrease as the crystal size decreases, indicating heterogeneous distribution of crystals' size suspensions.

Before and after each filtration the mass fraction of rubrene in the filtrate was measured by absorption (fig. 1.a).

By substracting the final absorbance from the initial absorbance, the mass fraction of the removed population and size distribution were deduced (fig. 2). The striking information is the correlation of **size** with **toluene over surfactant ratio**. Indeed as the proportion of surfactant in the emulsion increases, the size of the crystals decreases. For instance for the sample where the ratio is one to one, the percentage of sub-micrometer crystals is 40 %, and the percentage of crystals smaller than 25 nm is 8 %. Whereas for the sample with a ratio of 1 / 30, the percentage of sub-micrometer crystals is less than 5 %, and there are 70 % of crystals smaller than 25 nm.

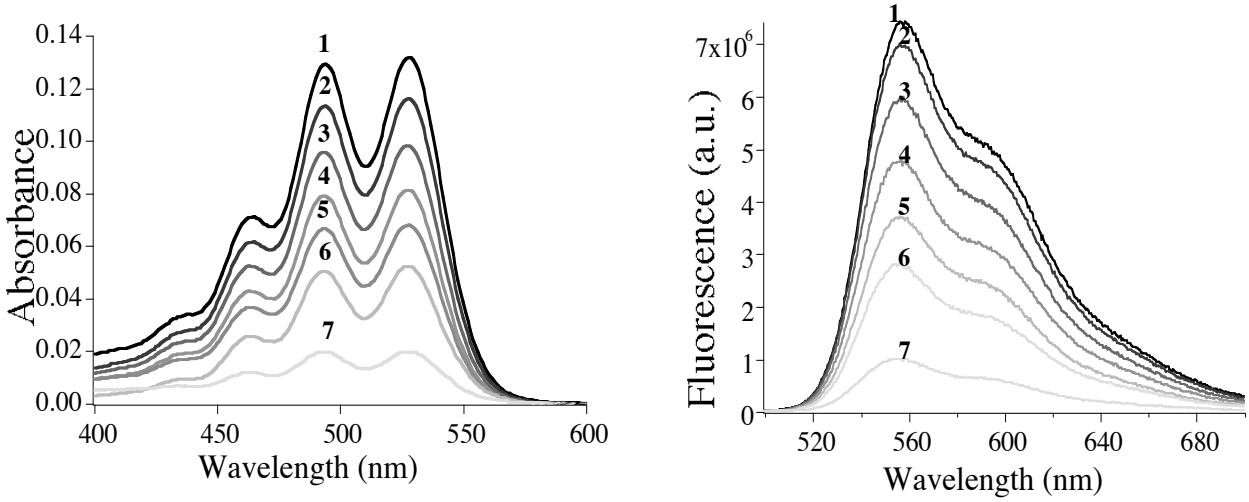

Figure 1 : Size control by filtration, studied by absorbance (figure1.a : left) and fluorescence measurements (figure 1.b : right). Pore size : **1** – no filtration, **2** – 0,80 µm, **3** – 0,45 µm, **4** – 0,22 µm, **5** – 0,10 µm, **6** – 0,05 µm, **7** – 0,025 µm.

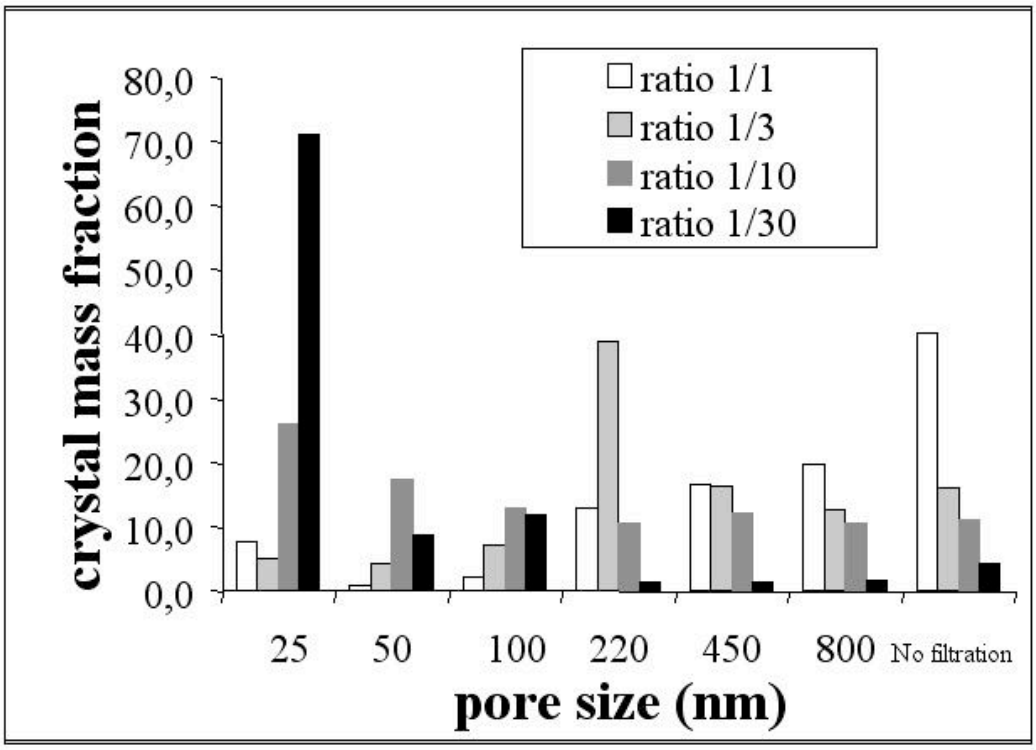

Figure 2 : Histogram of the crystal mass fraction as a function of pore size. The size depends on the ratio of toluene over surfactant. As the ratio decreases, the percentage of « small » crystals increases. In sample with ratio 1/30, the suspension contains mainly nanocrystals (size below 25 nm).

Thus we can produce crystals of nanometer sizes. And we have achieved to control and modulate the size thanks to the ratio of toluene over surfactant. In the following studies, we will mainly focus on crystals which size is less than 100 nm (filtration on 0.1 µm pore size).

3.2. Yield measurements on nanocrystals. Diffusion effect and shadow effect.

Absorption and fluorescent measurements on colloidal dispersion of nanoparticles of pigment are made difficult by their scattering and by local saturation of the absorption. Indeed, the very high absorption coefficient of dyes make that inside a 1 μm^3 volume, the front molecules completely shade the back ones. δ, the characteristic decay length of light intensity in an assembly of molecules is given by :

$$\delta^{-1} = 10^5 \varepsilon d / M = \varepsilon / (10 \mathcal{N} V)$$

where ε is the molar extinction coefficient in $mol^{-1}.L.cm^{-1}$;
d is the density of the crystal in $g.mL^{-1}$, d = 1,263 $g.mL^{-1}$ for rubrene [31];
M is the molecular weight in $g.mol^{-1}$;
$\mathcal{N}$ is the Avogadro number;
V is the molecule volume in m^3.

This gives a penetration depth of 500 nm for light inside rubrene, at 540 nm. This will affect the estimation of the total concentration of rubrene molecules in the suspensions when nanocrystals, larger than 150 nm, are present. Indeed the section of the cuvet is only partially occupied by nanocrystals and the transmitted intensity is given by :

$$I / Io = \iint 1 - 10^{-\varepsilon l(x,y)/10\mathcal{N}V} dxdy$$

Where x,y cover the section of the light beam *I*. *l(x,y)* is the dye thickness at the position x,y. This linearises if *l(x,y)* ε / (10 $\mathcal{N}$ V) < 0.1 for individual nanocrystals. This implies that for suspensions made of crystals below 150 nm in diameter, the average absorbance reflects the average dye concentration. Over 150 nm, the absorbance of rubrene nanocrystals will underestimate dye concentration. This effect depends on the molar extinction coefficient. Absorption at the peak wavelength will be saturated sooner than in the valley. This is shown on fig. 3 where the spectra of microcrystals are compared with the spectra of nanocrystals and molecules. In microcrystals, the absorbance peaks are levelled off and the band width is broadened.

Shadow effect, also affects fluorescence. The fluorescence photon is emitted in the crystal and it has a good probability to go through that crystal. Thus a suspension of microcrystals may exhibit inner filter effect even for solution of absorbance below 0.1. As seen on fig. 1b this inner filter effect is very limited for our rubrene samples.

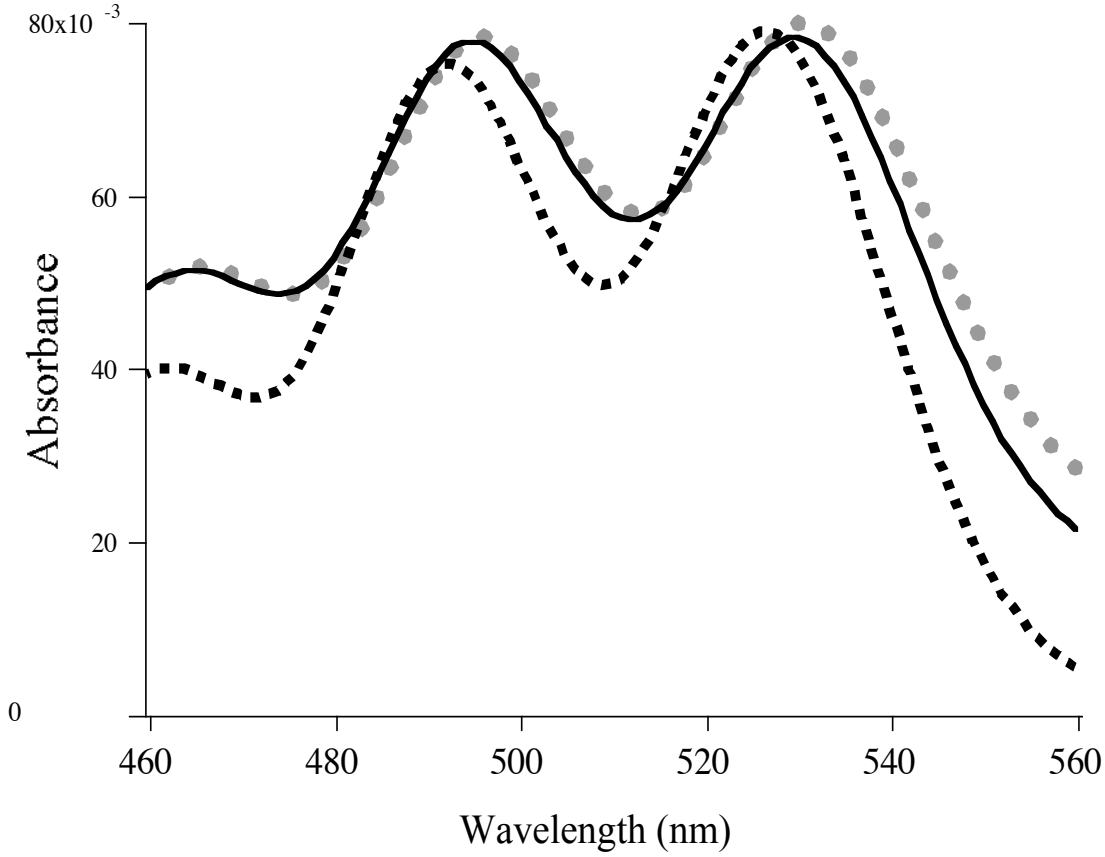

Figure 3 : Comparison of absorbance spectra of rubrene in toluene solution (black dotted curve), a nanocrystals suspension (black curve), a microcrystals suspension (grey dotted grey curve). A band broadening and a peak red-shift are observed.

In absence of an inner filter effect, the fluorescence yield is not affected by shadow effect. The fluorescence yield is the ratio of the amount of light emitted to the amount of light absorbed by the sample. This does not require the estimation of the concentration from the absorption spectrum. The fluorescence yield of a population of nanocrystals can be determined even if we do not know precisely their concentration nor the concentration of dyes in the solution.

3.3. Comparison of spectroscopic properties between rubrene in toluene and crystals suspensions. yield and lifetime in toluene.

Fluorescence quantum yield of rubrene in toluene under air was measured to be 0.61 using fluorescein as a reference. It reaches 0.90 when air is removed [32]. Fluorescence quantum yield in air of crystals suspensions was calculated as a function of crystal size (fig. 4).

As the microcrystals size decreases, the fluorescence quantum yield increases. For the smallest nanocrystals (25 nm in diameter), the fluorescence yield has a eighty percent value, which is better than the 0.61. But as the crystals size increases, the fluorescence quantum yield measured for the monomer in toluene decreases down to 0.1. This low fluorescence quantum yield of rubrene crystal and its sharp change at small size contrast with its high fluorescence lifetime. Fluorescence decay curves of rubrene in different phases are shown in fig.5. Rubrene in aerated toluene has a 10.3 ns lifetime (see fig.8), which is in perfect agreement with 0.61 fluorescence yield in presence of oxygen inhibition. For molecules, the removal of oxygen induces an increase of the fluorescence lifetime because of the reduction of intersystem crossing, and the suppression of a possible electron transfer pathway.

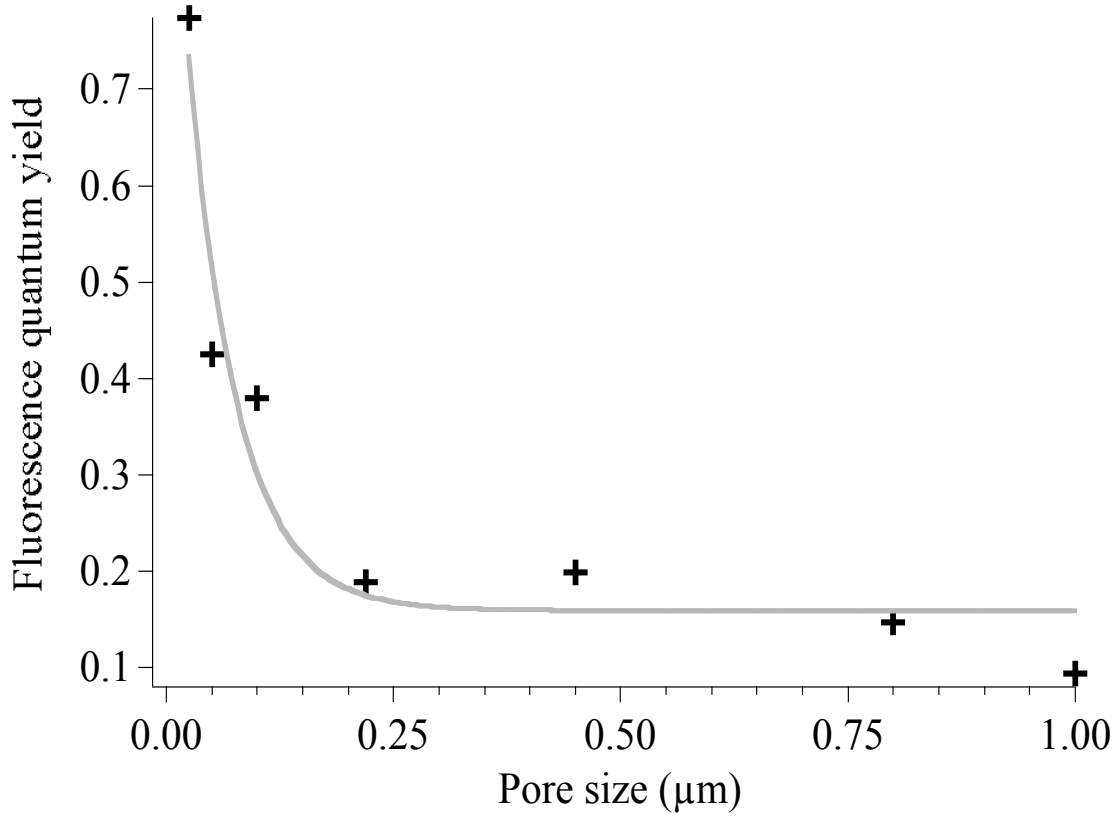

Figure 4 : Fluorescence quantum yield of crystals suspensions as a function of crystals size. The smaller the crystals are, the higher the yield is.

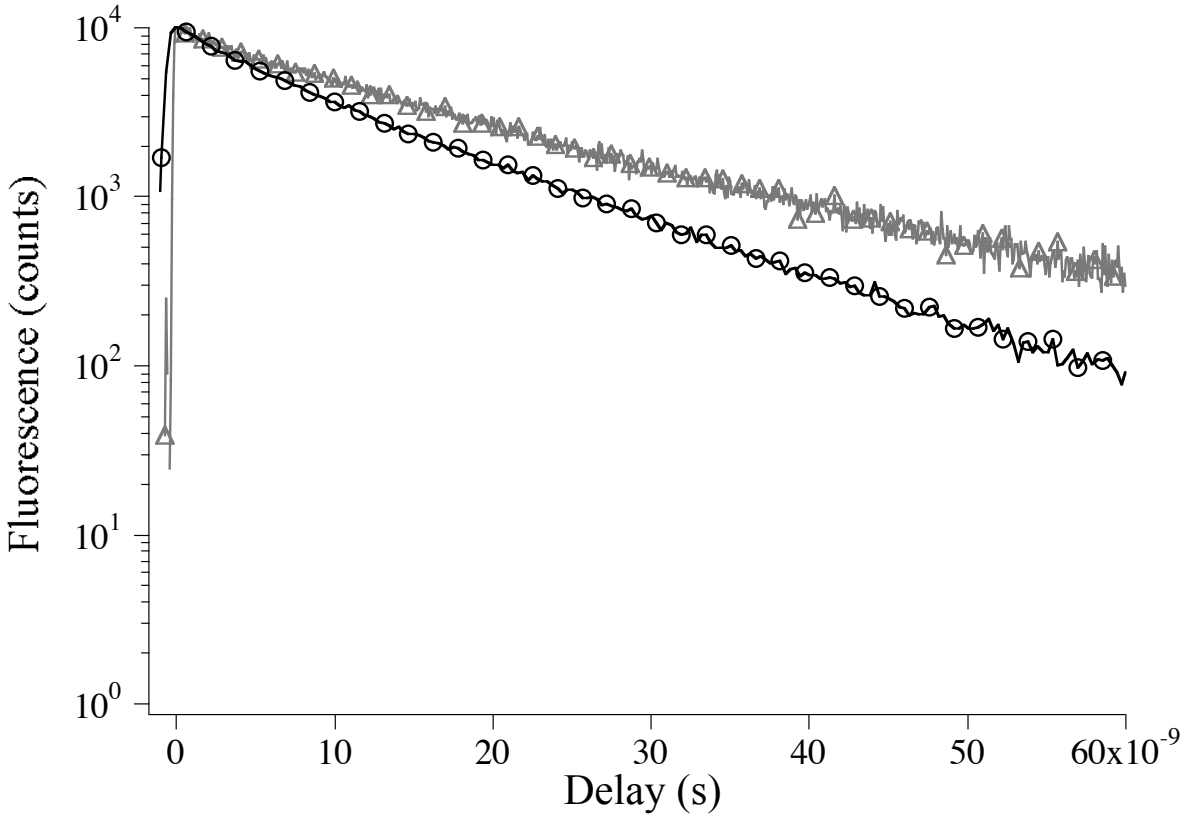

Figure 5 : Decay curves of rubrene nanocrystals suspension (0.1 µm filtration threshold - triangles), microcrystals suspension (no filtration - circles). Excitation : 494 nm – emission : band pass filter above 505 nm.

For nanocrystals, from the fluorescence lifetime of 16.4 ns, we can expect a fluorescence yield close to one. The contradiction can be resolved by the presence of dark crystals where a static quenching inhibits all fluorescence.

We assume that the defects or impurities that do fully inhibit fluorescence of a nanocrystal is a constant small fraction of rubrene κ. The probability for a crystal of n molecules to be fluorescent is given by :

$$(1-\kappa)^n \approx \exp(-n\kappa)$$

Thus the fluorescence yield will decrease exponentially with the volume of the nanocrystal. From the adjustment of fig. 4, we get a molar fraction of quenching defects per rubrene of 10^{-5}. Clearly defects in rubrene nanocrystals are not related to the surface as the fluorescence yield increases with the surface to volume ratio.

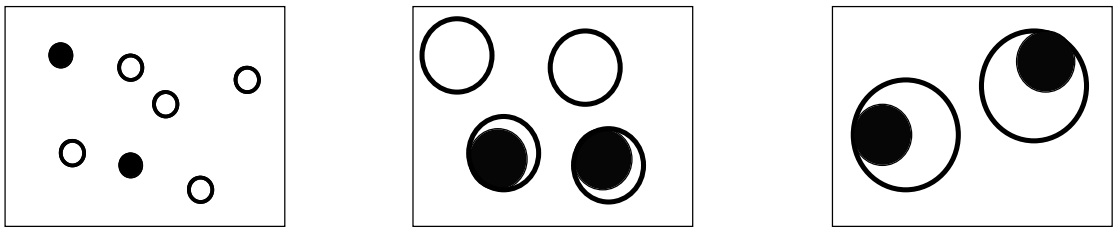

Less than 25 nm particles | Less than 100 nm particles | Less than 300 nm particles

Figure 6 : Interpretation of fluorescence behaviour (lifetime and quantum yield) with size. Hypothesis of the presence of an impurity.
When crystals' size is smaller than impurity, two populations of particles exist. One is totally quenched (black dots) and one exhibits total fluorescence (white dots). Behaviour of particles is close to that ofmonomer.
When size crystals is bigger than impurity, only one population can be considered. Then particles are quenched, lifetime and quantum yield decrease.

This increase of fluorescent yield as size decreases is not due to the increasing fraction of molecular rubrene. Rubrene is not soluble in water, even in presence of CTACl. Thus the spectroscopic signature of rubrene monomer in CTACl micelles where not obtained directly. But we can infer from the properties of the molecule in toluene solution that the quenching by oxygen will reduce the fluorescence lifetime and that the anisotropy of their fluorescence will be close to 0.4. The measured anisotropy is below 0.02 (data not shown) and no short component is seen in the fluorescence decay (Fig. 5). Thus nanocrystals suspensions only contain crystals and no residual monomers. Defects or impurities will fully inhibit fluorescence over a limited distance. At longer distances, it will take some time for the excitation to hop from dye to dye toward the defect. For these remote molecules the quenching will appear as a reduction of the fluorescence lifetime. Indeed in fig. 5, fluorescence lifetime of microcrystals (crushed crude powder) is 12.6 ns and that of nanocrystals is 16.4 ns.

The full scheme can be schematically explained on fig. 6. The very low value (0.1) of fluorescence quantum yield for microcrystals and the shorter lifetime can be explained by the presence of a defect, which quenches partially the emission (fig. 6). To explain the increase of yield with decreasing size, we can say that nanocrystals have a size smaller than the impurity (picture on the left, fig. 6). Two populations of nanocrystals exist : a fluorescent one (white dots) and a non-fluorescent one (black dots). This group do not emit light and do not participate to fluorescence decay and thus have no contribution to lifetime.

Concerning microcrystals, impurity is smaller than crystals size (picture on the right, fig.6). Then only one population of crystals can be considered and is partially quenched with a reduced lifetime.

3.4. Power effect on fluorescence lifetime.

The fluorescence yield of rubrene nanocrystals also depends on the laser power as shown in fig. 7. We have recorded the fluorescence intensity in a confocal set-up, where the sample was dilute enough to have only one particle at a time [33].

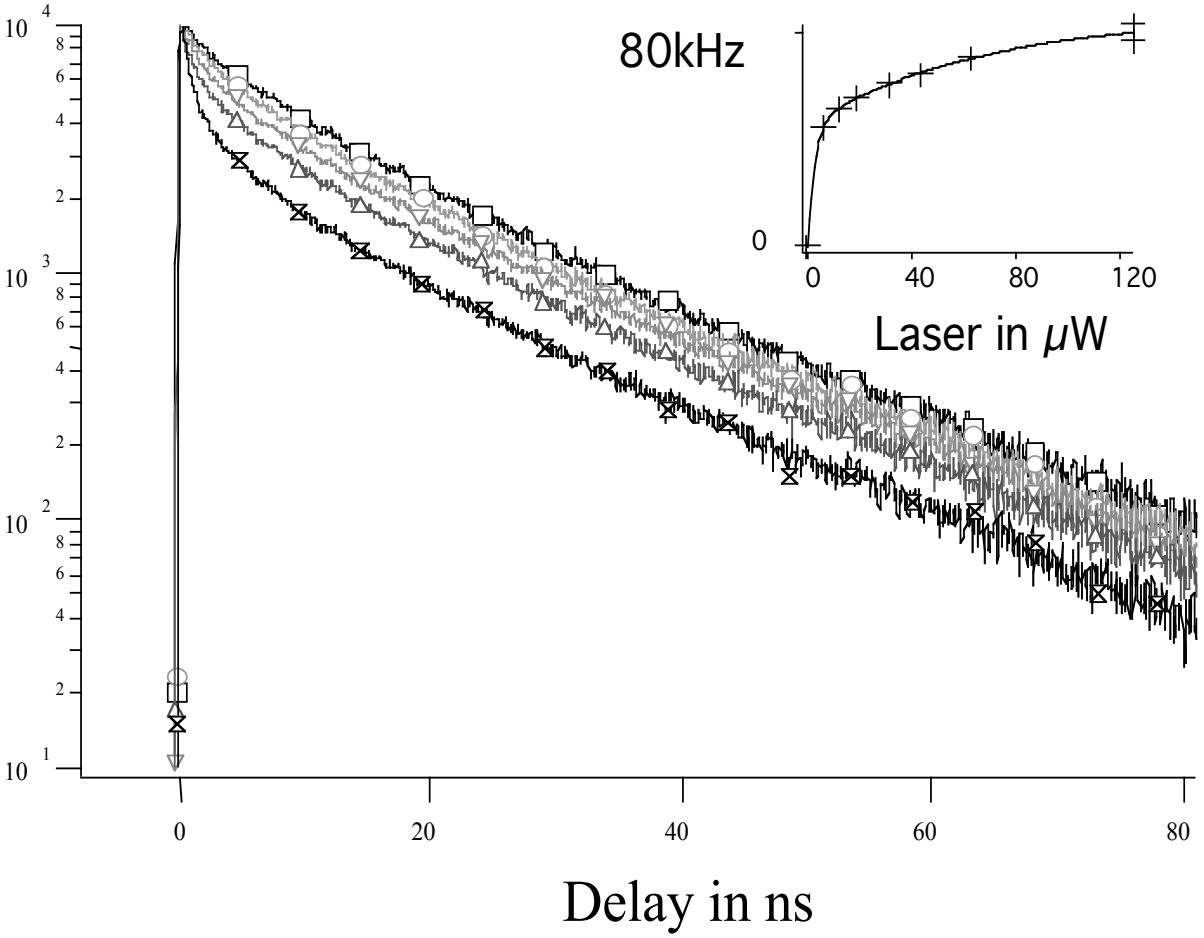

Figure 7 : fluorescence decays recorded at increasing laser power. The reduced fluorescence lifetime reflects the diffusion of the excited states inside the crystal that leads to their annihilation. This annihilation effect contributes to the saturation of fluorescence at high laser power shown in the inserted figure (upper right).

This saturation behaviour is seen for single molecules, where it is due to the saturation of the transition and to the accumulation of the molecules in the triplet manifold. In nanocrystals, this saturation can be due to the singlet-singlet annihilation and to the singlet-triplet annihilation. Indeed when two excited states are produced in vicinity they can diffuse and collide. The collision always leads to a reduction of the number of excited states [34].
A fast component in the fluorescence decay appears as the power of the laser is increased. This reduced fluorescence lifetime reflects the diffusion of the excited states inside the crystal that leads to their annihilation. The excited states produced in one part of the crystal act as quenchers for the fluorescence of the other molecules in the assembly. The long diffusion time observed implies that the sample was composed of relatively large crystals. As the laser power is increased the fraction of crystals where excited state annihilation occurs is increased and the fraction of the fast component is increased.
The triplet nature of the excited state that is involved in the annihilation is shown by the effect of oxygen on the fluorescence lifetime. On fig.8 we see a reduction of the fluorescence lifetime upon removal of oxygen for rubrene crystals suspension. At low laser power, oxygen does not reduce the fluorescence lifetime of rubrene nanocrystals. It does not interact with singlet excited states. But oxygen is known to kill triplet states. At high laser power the triplets accumulated in the crystal inhibit the fluorescence. Oxygen, by removing the triplet states, favours crystal fluorescence. At low laser power, the fluorescence lifetime of nano-crystal is longer than that of molecule dissolved in toluene.

The structure of the crystal protects the singlet-excited state from the oxygen. We have not measured the triplet lifetime of rubrene in crystal and in solution and the influence of oxygen on it. But we can infer that they are much longer than that of the singlet state. Even if the crystal structure protects the triplet state from oxygen like it protect singlet state, the longer lifetime of triplet give reason that it will not accumulate in presence of oxygen.

Defects and triplet states both act as quenchers dispersed in the crystal volume. They have a strong effect on fluorescence yield and also reduce the fluorescence lifetime. The crystal structure protects fluorescence from oxygen. At low power, the singlet-excited state is shielded from deactivation. At high laser power, oxygen quenches the quencher, the triplet state, and fluorescence is recovered.

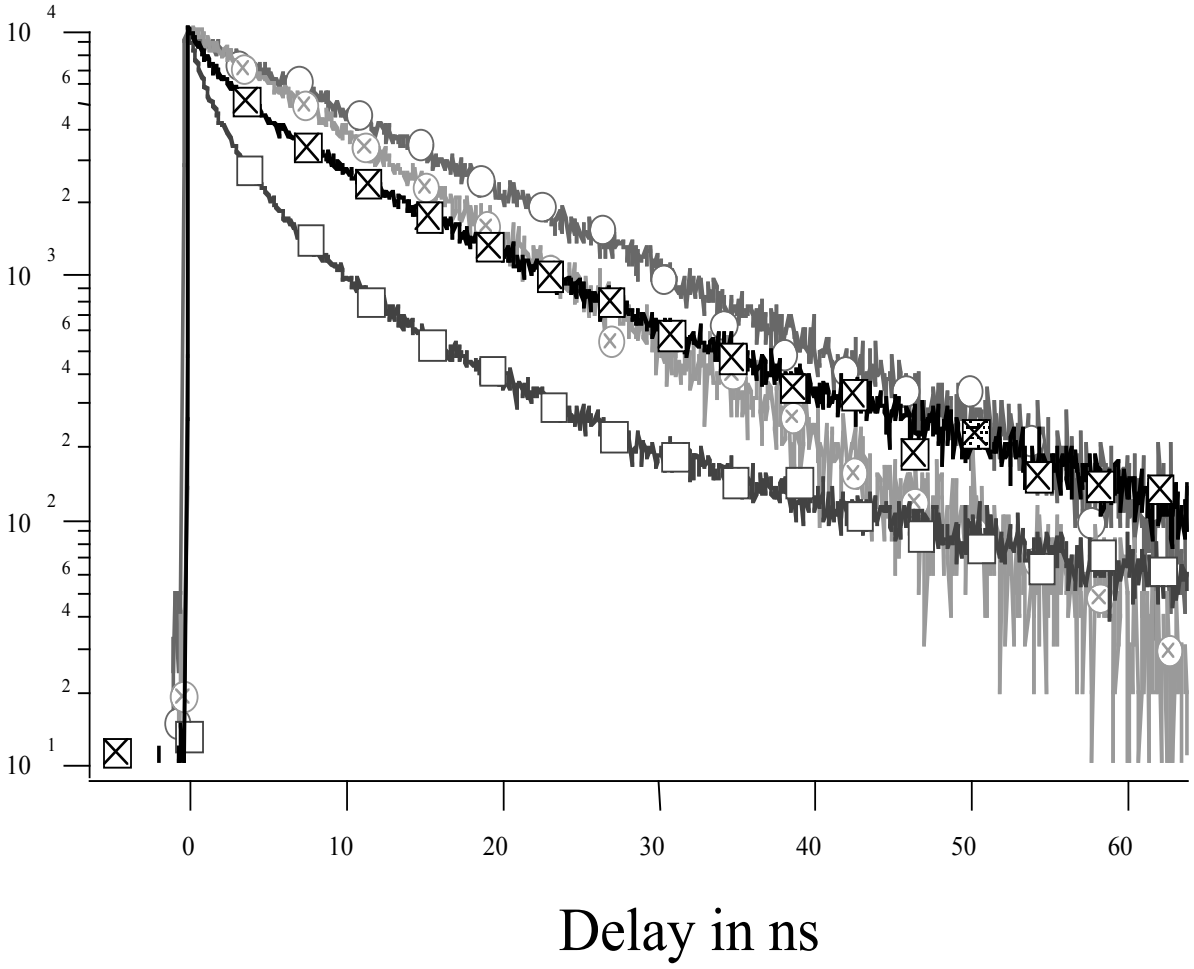

Figure 8 : Oxygen effect on fluorescence decay of rubrene.
In toluene : empty circles : No O_2 - circles and crosses : with O_2
Rubrene crystals suspension empty squares : No O_2 - squares and crosses : with O_2.

CONCLUSION

Rubrene nanocrystals exhibit a long lived fluorescence in air. The crystal structure protects singlet states from oxygen. But the fluorescence yield spans from 0.7 down to 0.08 decreasing as their size increases. Surface of rubrene nanocrystals does not create quenching defects. The low fluorescence yield is due to the presence of impurities that induce a static quenching of the fluorescence. Nanocrystals smaller than 50 nm have a high average fluorescence yield because of the low probability of presence of an impurity.

We have shown that the decrease of the fluorescence yield with the power of the excitation light and the amplification of the effect by removing oxygen are due to the Triplet-Singlet annihilation that inhibits fluorescence when more than one excited state is present in the nanocrystal.

We are able to produce crystals of nanometer sizes. And we have achieved to control and modulate the size thanks to the ratio of toluene over surfactant. The smaller the nanocrystals are, the more fluorescent they are.

REFERENCES

[1] E. Hanamura, Phys. Rev. B, 37 (1988) 1273.

[2] L.S. Li, A.P. Alivisatos, Advanced Materials, 15 (2003) 408.

[3] M. Dahan, T. Laurence, F. Pinaud, D.M. Chemla, A.P. Alivisatos, M. Sauer, S.Weiss, Optics L etters, 26 (2001) 825.

[4] B.Dubertret, P. Skourides, D.J. Norris, V. Noireaux, A.H. Brivanlou, A. Libchaber , Science, 298 (2002) 1759.

[5] W.J. Parak, D. Gerion, T. Pellegrino, D. Zanchet, C. Micheel, S.C. Williams, R. Boudreau, M.A. Le Gros, C.A. Larabell, A.P. Alivisatos, Nanotechnology (Bristol. Print), 14 (2003).

[6] D. Trau, R. Renneberg, Biosens. Bioelec., 18 (2003) 1491.

[7] D. Trau, W. Yang, M. Seydack, F. Caruso, N.T. Yu, R. Renneberg, Anal. Chem., 74 (2002) 5480.

[8] S. Forrest, MRS Bull. 26 (2001) 108.

[9] H. Kasai, H. S. Nalwa, H. Oikawa, S. Okada, H. Matsuda, N. Minami, H. Kakuta, K. Ono, A. Mukoh, H. Nakanishi, Jpn. J. Appl. Phys. 31 (1992) 1132.

[10] D. Xiao, W. Yang, H.B. Fu, Z. Shuai, Y. Fang, J.N. Yao, J. Am. Chem. Soc., 125 (2003) 6740.

[11] F. Bertorelle, D. Lavabre, S. Fery-Forgues, J. Am. Chem. Soc., 125 (2003) 6244.

[12] K. Baba, H. Kasai, S. Okada, H. Oikawa, H. Nakanishi, Jpn. J. Appl. Phys., 39 (2000) 1256.

[13] K. Baba, H. Kasai, S. Okada, H. Oikawa, H. Nakanishi, Optical Mat., 21 (2002) 591.

[14] H. Oikawa , T. Mitsui, T. Onodera, H. Kasai, H. Nakanishi, T. Seikiguchi, Jpn. J. Appl. Phys., 42 (2003) 111.

[15] T. Onodera, H. Kasai, S. Okada, H. Oikawa, K. Mitsuno, M. Fujitsuka, O. Ito, H. Nakanishi, Optical Mat., 21 (2002) 595.
[16] H.B. Fu,, B. H. Loo, D.B. Xiao, R.M. Xie, X.H. Ji, J.N. Yao, B.W. Zhang, L.O. Zhang, Angew. Chem. Int. Ed., 41 (2002) 962.
[17] Fu, H. B. and J. N. Yao, J. Am. Chem. Soc., 123 (2001) 1434.
[18] E. Botzung-Appert, N.T. Ha-Duong, P.L. Baldeck, R. Méallet-Renault, R.B. Pansu, A. Ibanez , Spatial distribution control of microscopic crystals, E.U. patent N° PCT / FR03 / 02072 (2003).
[19] N. Sanz, P. Terech, D. Djurado, B. Deme, A. Ibanez, Langmuir, 19 (2003) 3493.
[20] R. Méallet-Renault, P. Denjean, R.B. Pansu, Sensors and Actuators B, 59 (1999) 108.
[21] R. Méallet-Renault, H. Yoshikawa, Y. Tamaki, T. Asahi, R.B. Pansu, H. Masuhara, Polymer for Advanced Technologies, 11 (2000) 772.
[22] T. Förster, Disc.Faraday Soc., 27 (1959) 7.
[23] V. Balzani, P. Ceroni, S. Gestermann, M. Gorka, C. Kauffmann, F. Vögtle, Tetrahedron, 58 (2002) 629.
[24] L. Chen, et al., Proc. Nat. Acad. Sci. USA, 96 (1999) 12287.
[25] L. Liangde, R. Helgeson, R.M. Jones, D. McBranch, D. Whitten, J. Am. Chem. Soc., 124 (2002) 483.
[26] M. Pauchard, S. Huber, R. Méallet-Renault, H. Mass, R.B. Pansu, G. Calzaferri, Angewandte Chemie, 40 (2001) 2839.
[27] F. Treussart, E. Botzung-Appert, N.T. Ha-Duong, A. Ibanez, J.F. Roch, R.B. Pansu, Chem Phys Chem., 4 (2003) 757.
[28] T. Tsutsui, Nature 420 (2002) 752.
[29] A.K. Dutta, T.N. Mishra, A.J. Pal, Solid State Comm., 99 (1996) 767
[30] L. Schoutteten, P. Denjean, R. B. Pansu, Journal of Fluorescence, 7 (1997) 155.
[31] D. E. Henn, J. Appl. Cryst. 4 (1971) 256.
[32] J. B. Birks, (ed.) Photophysics of aromatic molecules, 1969.
[33] A. Tessier, R. Méallet-Renault, P. Denjean, D. Miller, R.B. Pansu, Phys. Chem. Chem. Phys., 1 (1999) 5767.
[34] J.P. Lemaistre, P. Reineker, M. Schreiber, R.S. Meltzer, Journal of luminescence, 76-77 (1998) 437.